Bioconjugate Chemistry

pubs.acs.org/bc

Article

Long-Acting Poly(ADP-ribose) Polymerase Inhibitor Prodrug for Humans

Christopher W. Carreras, Shaun D. Fontaine, Ralph R. Reid, Gary W. Ashley, and Daniel V. Santi*

Cite This: *Bioconjugate Chem.* 2024, 35, 551−558

Read Online

ACCESS | Metrics & More | Article Recommendations | Supporting Information

ABSTRACT: Poly(ADP-ribose) polymerase inhibitors (PARPi) have been approved for once or twice daily oral use in the treatment of cancers with BRCA defects. However, for some patients, oral administration of PARPi may be impractical or intolerable, and a long-acting injectable formulation is desirable. We recently developed a long-acting PEGylated PARPi prodrug, PEG~talazoparib (TLZ), which suppressed the growth of PARPi-sensitive tumors in mice for very long periods. However, the release rate of TLZ from the conjugate was too fast to be optimal in humans. We prepared several new PEG~TLZ prodrugs having longer half-lives of drug release and accurately measured their pharmacokinetics in the rat. Using the rates of release of TLZ from these prodrugs and the known pharmacokinetics of free TLZ in humans, we simulated the pharmacokinetics of the macromolecular prodrugs and released TLZ in humans. From several possibilities, we chose two conjugates that could be administered intravenously every 2 weeks and maintain TLZ within its known therapeutic window. We describe situations where the PEG~TLZ conjugates would find utility in humans and suggest how the intravenously administered long-acting prodrugs could in fact be more effective than daily oral administration of free TLZ.

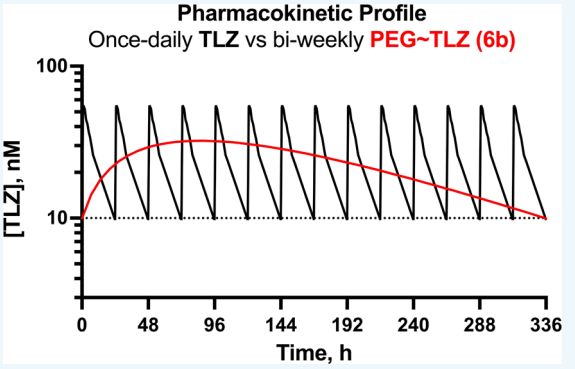

INTRODUCTION

Poly(ADP-ribose) polymerase (PARP) is a key component of DNA damage response (DDR). The enzyme binds to single-strand breaks of damaged DNA and recruits factors that repair the breaks.[1−3] Strand breaks that escape repair can form double-strand breaks that require homologous recombination repair (HRR) to avoid cell death. Hence, cells with defective HRR that arise from deficiencies in DDR proteins—such as BRCA1/2 and others[4,5]—rely on PARP and are highly sensitive to PARP inhibitors (PARPi) that cause synthetic lethality. Thus, PARPi target cancers with a deficient DDR and increase the sensitivity of DNA-damaging agents.[6,7]

To date, four PARPi have been approved for once or twice daily oral use in the treatment of human cancers.[5] As with any frequently dosed drug, PARPi exhibits high C_{max} values and high peak-to-trough excursions.[8] Thus, we and others have posited that a long-acting PARPi that provided sustained exposure and lower C_{max} and C_{max}/C_{min} might provide a more effective, less toxic therapeutic.[9−12]

We recently reported a long-acting PEGylated PARPi[10]—PEG~talazoparib (TLZ)—developed using a unique approach for half-life extension of therapeutics. In this approach, a drug is covalently tethered to a long-lived carrier by a linker that slowly cleaves by β-elimination to release the drug (Scheme 1).[13] The cleavage rate, k_1, is determined by the nature of an electron-withdrawing "modulator" (Mod) and is unaffected by enzymes or general acid/base catalysts. A carrier used for β-eliminative linkers is often a long-lived circulating macromolecule—such as high molecular weight polyethylene glycol (PEG).[13] For this purpose, 4-arm PEG_{40kDa}—a 15 nm diameter nanocarrier—may be optimal because smaller PEGs have shorter half-lives, while larger PEGs all show similar elimination rates.[14] The prodrug is usually eliminated with a $t_{1/2}$ similar to that for the carrier, and the apparent $t_{1/2}$ of the released drug is usually similar to the $t_{1/2}$ of the prodrug.[13]

Scheme 2 shows the *in vivo* fate of a PEG prodrug where k_1 is the cleavage rate of the conjugate, k_2 is the clearance rate of the released, free drug, and k_S is the elimination rate of the prodrug. Since macromolecules have different elimination rates in different species, a prodrug optimal for one will likely not be for another. In mice, renal elimination of a PEG_{40kDa} carrier has a $t_{1/2}$ of only ∼1 day compared to ∼2 days in the rat and ∼6 days in humans,[14] and renal elimination of the prodrug may occur before significant amounts of drug are released. Hence, the *in vivo* rate of drug release, k_1, from the prodrug and the

Received: March 11, 2024
Revised: March 18, 2024
Accepted: March 21, 2024
Published: April 9, 2024

Scheme 1. Drug Is Covalently Tethered to a Long-Lived Carrier by a Linker That Slowly Cleaves by β-Elimination to Release the Drug

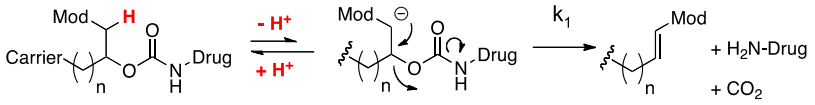

Scheme 2. *In Vivo* Fate of a PEG Prodrug

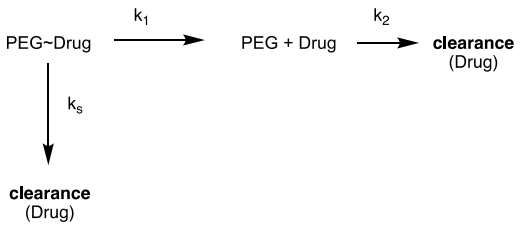

rate of prodrug elimination, k_s, must be balanced to achieve the desired pharmacokinetics in the intended target species.[15]

Previously, we applied this technology toward developing a long-acting PEG~TLZ prodrug suitable for use in murine preclinical models.[10] In mice, the macromolecular prodrug had a half-life of ~24 h, and remarkably, a single administration suppressed the growth of PARPi-sensitive tumors for very long periods. We wanted to translate these results to a PEG~TLZ that is useful for humans. However, the longer 6-day half-life of PEG_{40kDa} in humans requires a longer *in vivo* half-life of TLZ release to achieve this goal. We felt that the slower cleavage rates needed could be achieved using an appropriate modulator in the linker and an appropriate animal model for accurately determining the low k_1 values needed for the humanization of PEG~TLZ.

The objective of the present work was to design PEG~TLZ prodrugs with pharmacokinetics optimized for use in humans. Here, we (a) describe the synthesis and characterization of several PEG-TLZ prodrugs of TLZ that modify the rate of release of TLZ, (b) develop convenient and facile methods for analysis of the pharmacokinetics of the prodrug, (c) determine the *in vitro* and *in vivo* rates of drug release from PEG~TLZ prodrugs, and (d) simulate the pharmacokinetics of the TLZ conjugates and released TLZ in humans.

RESULTS

Synthesis and *In Vitro* Characterization of 4-Arm PEG_{40kDa}-TLZ Conjugates. The stable PEG~TLZ conjugate **1a** and releasable conjugate **1b** (Scheme 3) have straight-chain hydrocarbon linkers and were previously reported.[10] Releasable conjugates **6a**, **6b**, and **6c**, which contain a *gem*-dimethyl linker were prepared as described[16] and connected to $PEG_{40kDa}(CO_2Su)_4$ via an amide bond. *In vitro* rates of TLZ release from the releasable PEG_{40kDa}-TLZ conjugates (rPEG-

Scheme 3. Chemical Synthesis of PEG~TLZ Conjugates

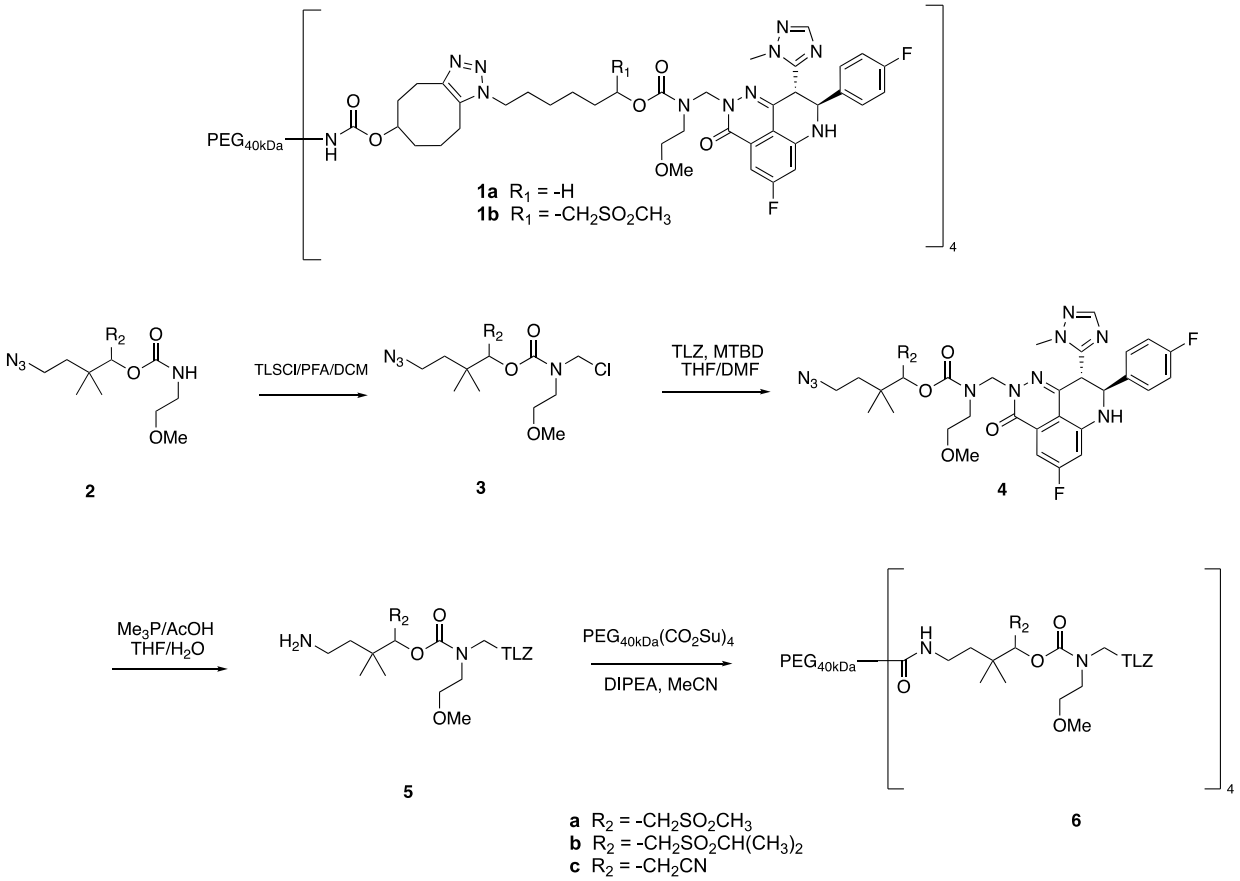

https://doi.org/10.1021/acs.bioconjchem.4c00112
Bioconjugate Chem. 2024, 35, 551−558

TLZ) at pH 9.4, 37 °C, and calculated to pH 7.4 gave $t_{1/2}$ values of 160 h for **1b**, 394 h for **6a**, 780 h for **6b** and 1780 h for **6c**.

Determination of the Rate of Drug Release from 1b in the Mouse vs Rat. We initiated this work by re-examination of the reported mouse pharmacokinetic data of rPEG~TLZ **1b** containing a $MeSO_2^-$ modulator.[10] The rate constant k_r for the disappearance of rPEG~TLZ from the plasma of the rat is the sum of the rates of prodrug cleavage and elimination, $k_r = k_1 + k_s$ (Scheme 2).[13] The rate constants k_s and k_r were reassessed as $k_s \sim 0.030 \pm 0.0021\ h^{-1}$, and $k_r \sim 0.033 \pm 0.0012\ h^{-1}$ to give a k_1 of $0.0028 \pm 0.0024\ h^{-1}$; as calculated by the square root of summation of squares the propagated error for k_1 was 85%, nearly as large as k_1 itself. Although k_1 is independent of the elimination rate, errors in determining k_1 from $k_r - k_s$ decrease with slower prodrug elimination—i.e., lower k_s. Hence, the problem with determining low k_1 values in mice is in part due to the high elimination rate of PEG_{40kDa} in the mouse, and can in part be ameliorated by using the rat where 4 arm PEG_{40kDa} has a longer elimination $t_{1/2,\beta}$ of about 2 days.[14]

The k_s of the rPEG~TLZ can be estimated by the elimination rate, k_s, of a corresponding stable PEG~TLZ conjugate (sPEG~TLZ), so k_1 may be calculated as $k_1 = k_r - k_s$. Pharmacokinetic parameters of PEG~TLZ conjugates **1a** and **1b** were determined independently in rats as described for mice.[10] Figure 1 shows the log *C* vs *t* profiles of **1a** and **1b** in

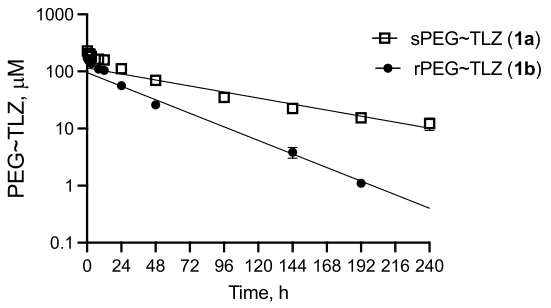

Figure 1. Pharmacokinetic profiles of **1a** (sPEG~TLZ) and **1b** (rPEG~TLZ) in the rat. Lines are a best fit of points obtained after 24 h to a single exponential decay model.

rats. As expected, k_r and k_s of **1a** and **1b** were slower in rats than in mice (Table 1) and the propagated error in k_1 decreased from 85% in the mouse to 17% in the rat. Hence, pharmacokinetic studies of all conjugates reported here were performed in the rats.

Pharmacokinetic Analysis. For some studies, we used our conventional method, termed the "difference method", to determine in elimination rates of rate constants (k_1) for *in vivo* linker cleavage; here, the elimination rates of both stable and releasable PEG~TLZs are individually determined and subtracted to obtain k_1.[13] We also developed a novel single-sample method that allows concurrent determination of pharmacokinetic parameters and determination of k_1 by a "ratio-metric method". The parameters attainable using the ratio-metric method include the elimination rates of rPEG~TLZ (k_r) and sPEG~TLZ (k_s), as well as the rate of linker cleavage (k_1) from rPEG~TLZ conjugates. The approach for the single-sample analysis was to administer a mixture of rPEG~TLZ and sPEG~TLZ to an animal and to analyze both conjugates in the same sample; *C* vs *t* profiles of the individual PEG~TLZs provide individual rates of elimination, while the ratio rPEG~TLZ/sPEG~TLZ vs *t* provides the rate of TLZ release from rPEG~TLZ.

For the ratio-metric analyses of pharmacokinetic parameters, we developed assays that would allow the determination of both rPEG~TLZ and sPEG~TLZ in the same sample. We showed that rPEG~TLZ **1b** could be completely converted to TLZ by treatment with NaOH (Figure 1A). A minor product, TLZ′, emerged from TLZ that reached ~20% of the TLZ + TLZ′ (Figure 1B), hereafter referred to as total TLZ or tTLZ; the tTLZ formed was constant from 5 min to 2 h, so it serves as a surrogate for the rPEG~TLZ originally present. In contrast to rPEG~TLZ, sPEG~TLZ was completely stable in 0.05 N NaOH for more than 2 h. Hence, rPEG~TLZ can be quantitatively converted to tTLZ by treatment with a base under conditions where sPEG~TLZ is inert.

In a sham experiment, mixtures of a constant amount of stable sPEG~TLZ **1a** and variable releasable rPEG~TLZ **1b** in acidified rat plasma/0.1 M citrate, pH 4.5 were analyzed by HPLC. As shown in Figure 2A, **1a** and **1b** elute as contiguous peaks. Following treatment with NaOH, sPEG~TLZ **1a** remained constant and the rPEG~TLZ **1b** was completely converted to TLZ (Figure 2B), confirming tTLZ is a good surrogate of **1b**. Figure 1C shows the relationship between the **1b**/**1a** ratio and rPEG~TLZ **1b**, validating the linearity of the ratio-metric method. Hence, PEG~TLZ in plasma samples containing both stable and releasable conjugates can be accurately determined upon treatment with a base.

Rats were administered a mixture of 15 μmol/kg sPEG~TLZ **1a** and 30 μmol/kg rPEG~TLZ **1b, 6a**, **6b**, or **6c**. Acidified and deproteinized plasma samples were analyzed by HPLC-fluorescence to quantitate the released free TLZ. Another portion of the clarified plasma was treated with NaOH, neutralized with AcOH, and analyzed by HPLC-UV for sPEG~TLZ (**1a**) and tTLZ serving as a surrogate of rPEG~TLZ. *C* vs *t* plots of sPEG~TLZ remaining after hydrolysis provided the elimination rate constant, k_s, (Figure

Table 1. Pharmacokinetic Parameters for PEG~TLZ Conjugates[a]

linker mod	stable **1a**		$MeSO_2^-$ **1b**		$MeSO_2^-$**1b**		GDM_2 $iPrSO_2^-$ **6b**		GDM_2 CN^- **6c**		GDM_2 $MeSO_2^-$ **6a**	
dose	30 μmol/kg **1a**		30 μmol/kg **1b**		30μmol/kg**1b**+15μmol/kg **1a**		30μmol/kg**6b**+15μmol/kg **1a**		30μmol/kg**6c**+15μmol/kg **1a**		30μmol/kg**6a**+15μmol/kg **1a**	
	mean	SD	mean	SD	mean	SD	mean	SD	mean	SD	mean	SD
k_s, h^{-1}	0.010	0.002			0.010	0.001	0.010	0.0008	0.010	0.0004	0.010	0.0002
k_r, h^{-1}			0.022	0.002	0.022	0.002	0.012	0.0002	0.010	0.0004	0.0014	0.007
k_1, h^{-1}[b]			0.012	0.002	0.012	0.002	0.0019	0.0008	0.00081	0.0006	0.0040	0.006
k_1, h^{-1}[c]					0.0093	0.001	0.0019	0.0007	0.00084	0.0002	0.0026	0.001

[a]*N* = 3 to 5 rats/group. [b]Measured by the difference method. [c]Measured by the ratio-metric method.

https://doi.org/10.1021/acs.bioconjchem.4c00112
Bioconjugate Chem. 2024, 35, 551−558

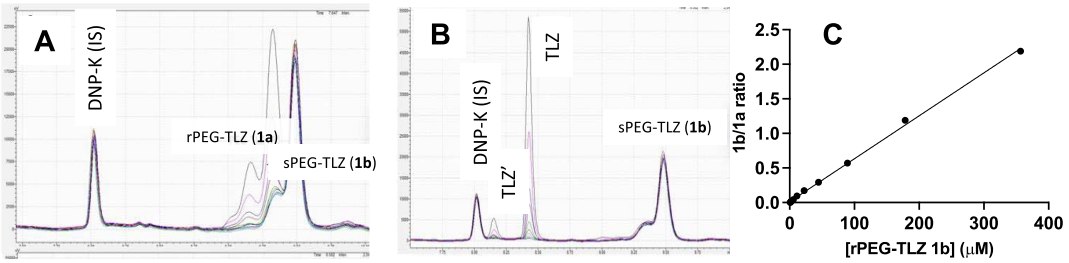

Figure 2. HPLC analyses of mixtures of PEG~TLZ **1a** and rPEG~TLZ **1b** before and after the base treatment. Protein-depleted samples of rat plasma contained 170 μM sPEG~TLZ and 0.3 to 360 μM rPEG~TLZ (A) before base-treatment, (B) 10 min after treatment in 0.05 N NaOH, and (C) rPEG~TLZ/sPEG~TLZ ratio vs the amount of rPEG~TLZ before NaOH cleavage.

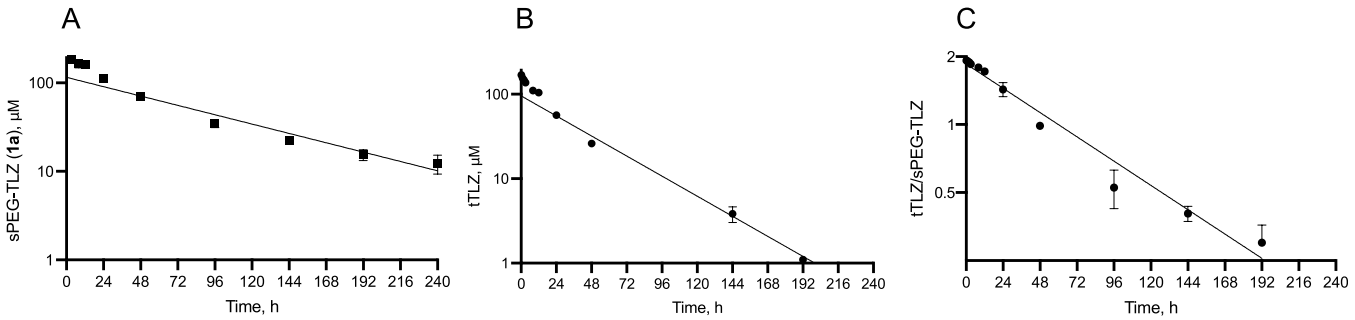

Figure 3. *C* vs *t* plots from the ratio-metric analysis of PEG~TLZ conjugates. (A) sPEG~TLZ **1a** remaining in plasma after NaOH hydrolysis. (B) tTLZ as proxy for rTLZ **1b** in plasma samples after NaOH hydrolysis, and (C) tTLZ/sPEG~TLZ **1a** as proxy for **1b**/**1a**.

3A), and plots of tTLZ released by hydrolysis (Figure 3B) provided the elimination rate constants, k_r, of rPEG~TLZ conjugates. Values for k_1 were then calculated from $k_1 = k_r - k_s$. Alternatively, the slope of the ln(tTLZ/sPEG~TLZ) peak area ratio vs *t* (Figure 3C) gave a direct estimate of k_1 since the ratio-metric method does not require exact quantitation of rPEG-TLZ and sPEG-TLZ.

The data obtained for pharmacokinetic analyses of PEG~TLZ conjugates are presented in Table 1. With single-agent **1b**, k_1 was calculated by the difference method; when **1a** was coadministered with another PEG~TLZ conjugate, k_1 values were calculated by both the difference and ratio-metric methods, which were in excellent agreement.

***In Vitro*–*In Vivo* Correlation of Rates of TLZ Release.** Figure 4 shows a plot of the *in vivo* vs *in vitro* $t_{1/2}$ values of the PEG~TLZ conjugates **1b**, **6a**, **6b**, and **6c**. There is an excellent *in vitro*–*in vivo* correlation with a slope of 0.5 (R^2 = 0.99).

Subcutaneous Injection of PEG~TLZ 1b. Previously, we showed that the terminal half lives of **1b** administered IP or IV to mice were identical.[10] Here, we determined the pharmacokinetics of 30 μmol/kg **1b** administered SC. Both IP and SC routes of administration showed the same pharmacokinetic profile and parameters for PEG~TLZ and released TLZ regardless of whether the 30 μmol/kg dose was delivered at 3.4 or 10 mL/kg (Figure S2, Table S1). We also compared the tumor growth inhibition of 30 μmol/kg **1b** administered as a single dose either IP or SC to MX-1 tumors; both gave complete growth inhibition for at least 40 d (Figure S3). Hence, the pharmacokinetics and antitumor effects of PEG~TLZ **1b** appear to be the same whether injected IV, IP, or SC.

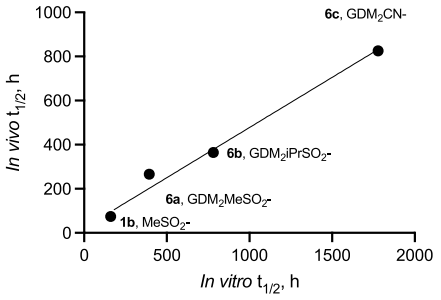

Figure 4. Correlation of *in vitro* and *in vivo* half-lives of releasable PEG~TLZ conjugates. *In vivo* half-lives were calculated from the rate constants obtained using the ratio-metric method (Table 1) and gave a slope of 0.5 with R^2 0.99.

Of concern with SC administration of **1b** was the possibility of injection site reactions. Histopathological examination of injection sites of the two groups of mice after completion of the pharmacokinetic experiment mostly showed changes in the epidermis including acanthosis and keratinization, as well as areas of inflammatory cells in the dermis (Table S2). These were attributed to persistent chronic trauma from rubbing, itching, and scratching of the skin. We concluded that injection site reactions were not particularly significant after the SC injection of **1b** in mice. However, we have no speculation on the toxicity of SC administration in larger animals.

Simulations in Humans. We desired a long-acting PEG~TLZ prodrug suitable for Q2Wk IV dosing, a common schedule for an IV-administered anticancer agent. The human QD dose of 1 mg TLZ/day shows a C_{max} of 55 nM and C_{min} of ~10 nM[17] which defines the upper and lower boundaries of the therapeutic window and indicates a safe and effective range to continuously maintain the plasma concentration of TLZ. We have previously described approaches to simulate the pharmacokinetics of releasable macromolecular prodrugs in humans using the species-independent cleavage rate obtained in animals and the pharmacokinetic parameters of the free drug in humans.[13] The equations for calculating the steady-state

https://doi.org/10.1021/acs.bioconjchem.4c00112
Bioconjugate Chem. 2024, 35, 551–558

Table 2. Simulated Steady-State Pharmacokinetic Parameters of TLZ Released from Q2Wk Dosing of PEG∼TLZ 1c and 5 Humans

conjugate	release $t_{1/2}$, h	TLZ, mg	PEG∼TLZ, mg	C_{max}, nM	C_{min}, nM	C_{max}/C_{min}	PEG∼TLZ utilization	AUC, nM/h
6a	267	43	1170	33	10	3.3	35%	7800
6b	365	49	1340	30	10	3.0	28%	7100

parameters with a chosen C_{min} and calculating the required dose to achieve the C_{min} have been reported[13] and are given in eqs S1 and S2. Using these equations, the reported elimination $t_{1/2}$ of 50 h and V_d of 5.2 L/kg for free TLZ[17] in humans, a prodrug elimination $t_{1/2}$ of 6 days[14] and the species-independent cleavage rates of PEG∼TLZ conjugates determined here, we estimated the human pharmacokinetic properties of the four PEG∼TLZ conjugates **1b**, **6a**, **6b**, and **6c** (Table S3). From these, we selected **6a** and **6b** because they have the most balanced properties, i.e., within the therapeutic window, acceptable dose, and utilization of prodrug—for Q2Wk dosing in humans (Table 2).

DISCUSSION

The objective of this work was to develop a long-acting PEG∼TLZ that would allow Q2Wk dosing in humans while maintaining TLZ within its therapeutic window. Although we previously reported a releasable PEG∼TLZ, the half-life of ∼70 h was too low for a Q2Wk dosing schedule in humans. In the present work, we describe (a) the synthesis and characterization of several PEG-TLZ prodrugs of TLZ with different release rates of TLZ, (b) a ratio-metric method for determining pro-drug and drug content of samples in a pharmacokinetic experiment, (c) the *in vivo* rates of drug release from the PEG∼TLZ prodrugs, and (d) simulations of the pharmacokinetics of the PEG∼TLZ in humans.

The synthesis of releasable PEG∼TLZ conjugates was achieved by the described methods.[10,16] In addition to conventional straight-chain linkers previously used,[10,16] we prepared conjugates with a new *gem*-dimethyl linker that inhibits the PEG-remnant remaining after drug release from undergoing undesirable Michael addition reactions.[16] Overall, the *in vitro* half-lives for TLZ release from the PEG∼TLZ conjugates spanned a ∼10-fold range of ∼160 to 1780 h.

Next, we determined the pharmacokinetics of the PEG∼TLZ conjugates to determine the *in vivo* rate of TLZ release. Here, we used rats in the study to mitigate errors resulting from the more rapid elimination of 40 kDa of PEG in mice. First, we developed an accurate ratio-metric method of analyzing pro-drug and drug content of samples in a pharmacokinetic experiment. Here, we administered a mixture of both stable and releasable PEG∼TLZ conjugates to the animal. Plasma samples were directly analyzed for released TLZ, and then treated with base to convert the remaining releasable PEG∼TLZ to TLZ. Then, a comparison of the released TLZ surrogate for releasable PEG∼TLZ to the stable TLZ at various times directly provides the rate of prodrug conversion to TLZ, k_1. This ratio-metric assay provided values for TLZ release rates with accuracy comparable to the more tedious, conventional assays previously used.

Having developed appropriate assays, the pharmacokinetics of each of the IV-administered PEG∼TLZ prodrugs was determined in the rat, primarily for the purpose of obtaining accurate rates of prodrug cleavage, k_1. As described above, k_1 values determined by either direct or ratio-metric assays were very similar. We obtained *in vivo* cleavage half-lives ranging from ∼50 to 800 h. Importantly, there was an excellent *in vitro*−*in vivo* correlation[18] of the half-lives with R^2= 0.99 which—because of the mechanism of β-eliminative linkers[19]—should extend to all species.

Finally, we addressed how the dosing schedules of the PEG∼TLZ conjugates might perform in humans. We previously described approaches to simulate the pharmacokinetics of macromolecular prodrugs in any species.[13] For this, we use the prodrug elimination rate and cleavage rate in a test animal, and the prodrug elimination rate and pharmacokinetic parameters of the free drug in humans.[13] We also require target blood levels of the drug in humans that will provide the desired therapeutic effect—usually, the levels obtained with the approved dosing schedule. With this information we optimized dosing schedules of the PEG∼TLZ so that over time the released TLZ never falls below the C_{min}—to maintain efficacy—or exceeds the C_{max}—to avoid toxicity; that is, the active-free drug always remains within the therapeutic window.

The approved human daily dose of TLZ shows a C_{min} of ∼10 nM and C_{max} of 55 nM[17] which defines the upper and lower boundaries of the therapeutic window. Constraining the TLZ levels within the therapeutic window, we estimated the human pharmacokinetic properties of the four releasable PEG∼TLZ conjugates studied here when dosed IV QWk, Q2Wk, or Q3Wk. The QWk dose was deemed unacceptable because of patient convenience and compliance, and the Q3Wk dosing required the administration of impractical amounts of prodrug. We, therefore, selected Q2Wk administration of two prodrugs, **6a** and **6b,** because they have the most balanced properties—i.e., remain within the therapeutic window, and acceptable dosing and utilization of prodrug—for dosing in humans. The TLZ released from appropriate doses of these prodrugs maintains the desired C_{min} of 10 nM and a low C_{max} of only ∼30 nM—∼50% of the C_{max} of QD TLZ. Also, the peak-to-trough excursion (C_{max}/C_{min} ∼ 3) for the released TLZ is significantly lower than that of QD TLZ (C_{max}/C_{min} ∼ 5.5) and only occurs every 2 weeks (Figure 5). Taken together, although PEG∼TLZ suffers from requiring IV administration, the pharmacokinetics of the released TLZ appears to be superior to those of QD TLZ.

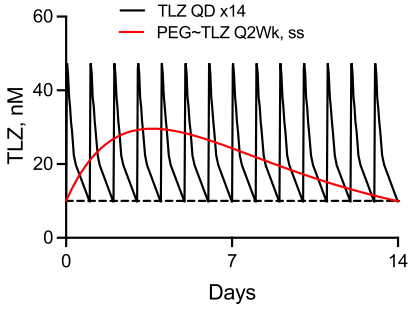

Figure 5. Comparison of the human PK profile of a daily PO 1 mg TLZ vs 49 mg of TLZ delivered via Q2Wk IV administration of **6b**.

https://doi.org/10.1021/acs.bioconjchem.4c00112
Bioconjugate Chem. 2024, 35, 551−558

An important question is why would one administer IV PEG∼TLZ when several QD oral PARP inhibitors are approved?

First, an IV-administered PARPi could offer an important option in situations where everyday oral administration may be impractical or intolerable. As examples: oral PARPi treatment may not be tolerable in patients with abdominal cancer who have had surgical procedures and consequent malabsorption or dumping syndrome; functional bowel obstruction in the setting of peritoneal carcinomatosis may not allow oral absorption of drugs; and patients with head and neck cancer with esophageal strictures may not be able to swallow oral medications.

Second, an IV-administered long-acting PEG−PARPi prodrug may, in fact, be more effective than daily oral administration of the free PARPi. For example, the prolonged exposure and low C_{max} and C_{max}/C_{min} that can be afforded by a very long-acting PEG∼TLZ might provide a more effective, less toxic therapeutic. Also, it should be possible to increase the dose of Q2Wk PEG∼TLZ almost 2-fold and still maintain TLZ within the C_{max}/C_{min} defined therapeutic window by QD TLZ; this would increase tumor exposure, which could very well increase efficacy. Finally, tumor accumulation of the prodrug—as observed in mouse tumors by an EPR effect[10,20]—should not be essential for efficacy in humans but, if present, would provide therapeutic benefits of tumor targeting and accumulation over and above what is possible for free TLZ. Hence, we posit that a Q2Wk dose of a properly designed IV-administered PEG∼TLZ would be at least as efficacious and possibly superior to daily oral TLZ in humans.

MATERIALS AND METHODS

General Methods. PEG_{40kDa}-$[NH_2]_4$ (Sunbright PTE-400PA) was purchased from SinoPEG, and TLZ was purchased from Medkoo (Morrisville, NC). All other commercially available chemicals were reagent grade and used without further purification. TLZ and PEG∼TLZ (**1a**, **1b**, **6a**, **6b**, and **6c**) were quantified by UV absorbance using $\varepsilon_{310\ nm}$ = 9872 M^{-1} cm^{-1}. Doses of PEG∼TLZ are reported with respect to the amount of TLZ delivered. HPLC analyses were performed on a Shimadzu LC-20AD HPLC system equipped with an SPD-M20A diode array detector and RF-10AXL fluorescence detector using a Phenomenex Jupiter 5 μm C18 column 300 Å (150 × 4.6 mm) and a mobile phase of H_2O/0.1% TFA and MeCN/0.1% TFA. UV−vis data were acquired on a Hewlett-Packard 8453 UV−vis spectrometer. MS analyses were obtained at the UCSF Small Molecule Discovery Center by ES^+/TOF mass spectrometry using a Waters Xevo G instrument with an Aquity solvent delivery system.

Chemical Synthesis. Synthesis of stable PEG∼TLZ (**1a**) and PEG-$[(5HCO/N_3)$-L(SO_2Me)NR-CH_2-TLZ$]_4$ (**1b**) were as previously described.[10] Amide connections were made by coupling $PEG_{40kDa}(CO\text{-}HSE)_4$ with NH_2-linker-TLZ.[15] Detailed synthesis and characterization of **6a**, **b**, and **c** and synthetic intermediates are presented in the Supporting Information.

*General Procedure for the Preparation of Azido-Linker-Carbamates (**2a**, **b**, **c**).* Requisite linker-HSCs were prepared according to a previously reported method.[16] This procedure is based on a previously reported method.[10] A round-bottom flask equipped with a stir bar, rubber septa, and nitrogen inlet was charged with appropriate linker-HSC (1.0 equiv), MeCN, and methoxy ethylamine (1.2 equiv). The reaction mixture was stirred at ambient temperature while iPr_2NEt (1.5 equiv) was added dropwise via syringe. The reaction mixture was stirred at 0 °C for 5 min and stirred at ambient temperature for 30 min. The reaction mixture was diluted with EtOAc (30 mL) and 5% aq $KHSO_4$ (30 mL). The aqueous phase was separated and extracted with EtOAc. The combined organic phases were washed with brine, dried over $MgSO_4$, filtered, and concentrated.

*General Procedure for the Preparation of Chloromethyl Carbamate (**3a**, **b**, **c**).* Azido-linker carbamates were reacted with TMSCl (4 equiv) and paraformaldehyde in DCE at 50 °C according to previously reported procedures.[10] After concentration, filtration, and trituration as described, the crude products were dissolved in THF to afford ∼0.5 M solutions and were used immediately without further purification.

*General Procedure for the Preparation of Azido-Linker-TLZ Conjugates (**4a**, **b**, **c**).* A 25 mL flask equipped with a stir bar, rubber septum, and nitrogen inlet was charged with TLZ (0.93 mmol), DMF (9.3 mL), and MTBD (1.12 mmol). The reaction mixture was cooled at 0 °C and a solution of linker chloromethyl carbamate (0.45 M in THF, 3.1 mL, 1.40 mmol, 1.5 equiv) was added rapidly via a syringe. The reaction mixture was stirred at 0 °C for 2 h. Reaction progress was monitored by C18 HPLC and was quenched when no further conversion was observed. The reaction mixture was cooled to −78 °C and diluted with 0.1 M Tris (pH 7.4). The semifrozen reaction mixture was allowed to warm with vigorous stirring and diluted with EtOAc and 0.1 M Tris. The aqueous phase was separated and extracted with EtOAc. The combined organic phases were washed with brine, dried over $MgSO_4$, filtered, and concentrated to afford a yellow oil.

*General Procedure for the Preparation of Amino-Linker-TLZ Conjugates (**5a**, **b**, **c**).* Azido-linker-TLZ (1 equiv) was dissolved in THF (0.1 M final concentration), and AcOH (2.5 equiv) was added. The reaction mixture was cooled at 0 °C, while a solution of Me_3P (1 M in THF, 5 equiv) was added via syringe. The reaction mixture was cooled at 0 °C for 4 h. H_2O (1 mL) was added, and the reaction mixture was stirred at 0 °C for 30 min. The reaction mixture was concentrated and redissolved in 3 mL of DMF. The resulting solution of crude product was purified via preparative C18 HPLC (25−70%B). The purified product was dissolved in MeCN (2 mL) and [TLZ] content was determined at A310:68.9 mM (138 μmol, 86% yield). The solution was stored at −80 °C until ready to use.

*General Procedure for the Preparation of PEG_{40kDa}-(Linker-TLZ)$_4$ Conjugates (**6a**, **b**, **c**).* Amino-linker-TLZ (1.3 equiv) and PEG-$(OSu)_4$ (1.0 equiv) in MeCN (13 mM final concentration) were treated with iPrNEt (10 equiv). The reaction mixture was stirred at ambient temperature for 0.5 h, concentrated, dissolved in THF, and added to 50% iPrOH/MTBE with stirring. The solids were collected by centrifugation and washed with 50% iPrOH/MTBE, MTBE.

***In Vitro* Drug Release Kinetics.** Solutions of PEGylated conjugates at pH 1.1 to 9.4 were kept at 37 °C in an HPLC autosampler. At appropriate intervals, aliquots were injected into a C18 HPLC column and eluted with a gradient of H_2O and MeCN containing 0.1% TFA. Peak areas measured by UV−vis were normalized against an internal standard, and data was fitted to a single-phase exponential equation.

Determination of *In Vivo* Release Rates of TLZ from PEG∼TLZ Conjugates.

https://doi.org/10.1021/acs.bioconjchem.4c00112
Bioconjugate Chem. 2024, 35, 551−558

1. *Drug administration*. Pharmacokinetic studies were performed at Murigenics (Vallejo, CA). Solutions of PEG∼TLZ were prepared in isotonic acetate (pH 5), sterile filtered through a 0.2 μm syringe filter, and TLZ content was determined by UV−vis (ε_{310nm} = 9872 $M^{-1}cm^{-1}$). Female Sprague−Dawley rats outfitted with jugular vein catheters were dosed with PEG∼TLZ conjugates. In the first cohort groups of rats (N = 4) were intravenously administered either stable PEG∼TLZ (**1a**, 15 μmol/kg), PEG-[amide-(Mod=Me-SO_2)-TLZ]$_4$ (**1b**, 30 μmol/kg), or a 2:1 mixture of **1a** and **1b** at 30 and 15 μmol/kg, respectively. In a second cohort, groups of rats (N = 3−5) were intravenously administered either a 2:1 mixture of **1a** and **6a**, **1a** and **6b**, or **1a** and **6c** (30 and 15 μmol/kg). Blood samples were collected at 0.17, 1, 2, 4, 8, 12, 24, 48, 96, 144, 192, and 240 h into K-EDTA tubes and combined with 1/10th volume 1 M citrate pH 4.5. Plasma samples were stored at −80 °C until analysis.
2. *HPLC Analysis of TLZ and PEG∼TLZ conjugates*. Plasma samples were analyzed for PEG∼TLZ and released TLZ by C18 HPLC. A 10 μL aliquot of each plasma sample was combined with an equal volume of mouse plasma containing 100 mM citrate, pH 4.5, and 35 μM DNP-lysine internal standard. Acetonitrile (60 μL) was added to the mixture, which was vortexed 10s and clarified by centrifugation. Portions of the supernatant (50 μL) were transferred to a 96-well plate and 150 μL of 0.33% acetic acid was added—these samples were used to assess free plasma TLZ. Separate portions of the supernatant (50 μL) were treated with 0.1 M NaOH to release TLZ from the releasable PEG∼TLZ conjugate. Following incubation at room temperature the samples were neutralized with 0.5% acetic acid. These samples were used to assess the concentration of stable PEG∼TLZ and released TLZ as a proxy for plasma releasable PEG∼TLZ. Samples were injected into a Phenomenex Jupiter C18 300 Å (150 × 4.6 mm) column heated to 40 °C and eluted with H_2O/MeCN/0.1% TFA (0−100% B over 15 min). Eluted TLZ and PEG∼TLZ conjugates were monitored at 310 nm fluorescence (λ_{ex} 310 nm; λ_{em} 460 nm).

Subcutaneous Administration of PEG∼TLZ (1b).

1. *Pharmacokinetics*. Two groups of CD-1 mice (N = 4/group) received a single SC dose of 30 μmol/kg PEG∼TLZ by injection of either an 8.9 mM solution at 3.4 mL/kg or a 3.0 mM solution at 9.9 mL/kg. Blood samples were obtained periodically via serial tail-snip, immediately treated with a 1 M citrate/0.1% pluronic F68 (pH 4.5) solution (10% of blood volume), and centrifuged to give plasma samples. Analysis of TLZ and PEG∼TLZ in plasma was performed as described above.
2. *Histology*. At the end of the PK study, animals were euthanized and the injection site was harvested, fixed in formalin, and transferred to 70% EtOH until H&E analysis.
3. *Antitumor efficacy in MX-1 xenografts*. Female scid mice (N = 6/group) bearing MX-1 tumors ∼150 mm^3 in size received a single dose of 30 μmol/kg PEG∼TLZ (2.9 mM at 10 mL/kg) by either IP or SC administration. Tumor volumes and body weights were measured twice weekly. MX-1 was verified to be free of mycoplasma and its identity was verified by genotyping at IDEXX (Fremont, CA).

■ ASSOCIATED CONTENT

Supporting Information

The Supporting Information is available free of charge at https://pubs.acs.org/doi/10.1021/acs.bioconjchem.4c00112.

Detailed procedures for chemical synthesis, additional pharmacokinetic, and pharmacodynamic data (PDF)

■ AUTHOR INFORMATION

Corresponding Author

Daniel V. Santi − *ProLynx, Inc., San Francisco, California 94107, United States;* orcid.org/0000-0002-3790-0673; Email: Daniel.V.Santi@prolynxinc.com

Authors

Christopher W. Carreras − *ProLynx, Inc., San Francisco, California 94107, United States;* orcid.org/0000-0001-7360-2350

Shaun D. Fontaine − *ProLynx, Inc., San Francisco, California 94107, United States*

Ralph R. Reid − *ProLynx, Inc., San Francisco, California 94107, United States*

Gary W. Ashley − *ProLynx, Inc., San Francisco, California 94107, United States*

Complete contact information is available at: https://pubs.acs.org/10.1021/acs.bioconjchem.4c00112

Notes

The authors declare the following competing financial interest(s): The authors are option or shareholders of ProLynx, Inc.

■ ACKNOWLEDGMENTS

The authors are grateful to Dr. Hyunil Jo (UCSF) for assistance in obtaining NMR spectra.

■ REFERENCES

(1) Murai, J.; Huang, S. N.; Das, B. B.; Renaud, A.; Zhang, Y.; Doroshow, J. H.; Ji, J.; Takeda, S.; Pommier, A. Trapping of PARP1 and PARP2 by Clinical PARP Inhibitors. *Cancer Res.* **2012**, *72*, 5588−5599.

(2) Murai, J.; Huang, S. N.; Ranaud, A.; Zhang, Y.; Ji, J.; Takeda, S.; Morris, J.; Teicher, B.; Doroshow, J. H.; Pommier, Y. Stereospecific PARP trapping by BMN 673 and comparison with olaparib and rucaparib. *Mol. Cancer Ther.* **2014**, *13*, 433−443.

(3) Groelly, F. J.; Fawkes, M.; Dagg, R. A.; Blackford, A. N.; Tarsounas, M. Targeting DNA damage response pathways in cancer. *Nat. Rev. Cancer* **2023**, *23*, 78−94.

(4) Lord, C. J.; Ashworth, A. BRCAness revisited. *Nat. Rev. Cancer* **2016**, *16*, 110−120.

(5) Lord, C. J.; Ashworth, A. PARP inhibitors: Synthetic lethality in the clinic. *Science* **2017**, *355*, 1152−1158.

(6) Stewart, R. A.; Pilie, P. G.; Yap, T. A. Development of PARP and Immune-Checkpoint Inhibitor Combinations. *Cancer Res.* **2018**, *78*, 6717−6725.

(7) Drean, A.; Lord, C. J.; Ashworth, A. PARP inhibitor combination therapy. *Crit Rev. Oncol Hematol* **2016**, *108*, 73−85.

(8) Bruin, M. A. C.; Sonke, G. S.; Beijnen, J. H.; Huitema, A. D. R. Pharmacokinetics and Pharmacodynamics of PARP Inhibitors in Oncology. *Clin Pharmacokinet* **2022**, *61*, 1649−1675.

(9) van de Ven, A. L.; Tangutoori, S.; Baldwin, P.; Qiao, J.; Gharagouzloo, C.; Seitzer, N.; Clohessy, J. G.; Makrigiorgos, G. M.;

Cormack, R.; Pandolfi, P. P.; Sridhar, S. Nanoformulation of Olaparib Amplifies PARP Inhibition and Sensitizes PTEN/TP53-Deficient Prostate Cancer to Radiation. *Mol. Cancer Ther* **2017**, *16*, 1279−1289.
(10) Fontaine, S. D.; Ashley, G. W.; Houghton, P. J.; Kurmasheva, R. T.; Diolaiti, M.; Ashworth, A.; Peer, C. J.; Nguyen, R.; Figg, W. D.; Beckford-Vera, D. R.; Santi, D. V. A Very Long-Acting PARP Inhibitor Suppresses Cancer Cell Growth in DNA Repair-Deficient Tumor Models. *Cancer Res.* **2021**, *81*, 1076−1086.
(11) Baldwin, P.; Likhotvorik, R.; Baig, N.; Cropper, J.; Carlson, R.; Kurmasheva, R.; Sridhar, S. Nanoformulation of Talazoparib Increases Maximum Tolerated Doses in Combination With Temozolomide for Treatment of Ewing Sarcoma. *Front. Oncol.* **2019**, *9*, 1416.
(12) Zhang, D.; Baldwin, P.; Leal, A. S.; Carapellucci, S.; Sridhar, S. A nano-liposome formulation of the PARP inhibitor Talazoparib enhances treatment efficacy and modulates immune cell populations in mammary tumors of BRCA-deficient mice. *Theranostics* **2019**, *9*, 6224−6238.
(13) Santi, D. V.; Schneider, E. L.; Reid, R.; Robinson, L.; Ashley, G. W. Predictable and tunable half-life extension of therapeutic agents by controlled chemical release from macromolecular conjugates. *Proc. Natl. Acad. Sci. U. S. A.* **2012**, *109*, 6211−6216.
(14) Sharda, N.; Khandelwal, P.; Zhang, L.; Caceres-Cortes, J.; Marathe, P.; Chimalakonda, A. Pharmacokinetics of 40 kDa Polyethylene glycol (PEG) in mice, rats, cynomolgus monkeys and predicted pharmacokinetics in humans. *Eur. J. Pharm. Sci.* **2021**, *165*, No. 105928.
(15) Fontaine, S. D.; Hann, B.; Reid, R.; Ashley, G. W.; Santi, D. V. Species-specific optimization of PEG∼SN-38 prodrug pharmacokinetics and antitumor effects in a triple-negative BRCA1-deficient xenograft. *Cancer Chemother Pharmacol* **2019**, *84*, 729−738.
(16) Hearn, B. R.; Fontaine, S. D.; Schneider, E. L.; Kraemer, Y.; Ashley, G. W.; Santi, D. V. Attenuation of the Reaction of Michael Acceptors with Biologically Important Nucleophiles. *Bioconjug Chem.* **2021**, *32*, 794−800.
(17) de Bono, J.; Ramanathan, R. K.; Mina, L.; Chugh, R.; Glaspy, J.; Rafii, S.; Kaye, S.; Sachdev, J.; Heymach, J.; Smith, D. C.; et al. Phase I, Dose-Escalation, Two-Part Trial of the PARP Inhibitor Talazoparib in Patients with Advanced Germline BRCA1/2 Mutations and Selected Sporadic Cancers. *Cancer Discov* **2017**, *7*, 620−629.
(18) Lu, Y.; Kim, S.; Park, K. *In vitro-in vivo* correlation: perspectives on model development. *Int. J. Pharm.* **2011**, *418*, 142−148.
(19) Schneider, E. L.; Henise, J.; Reid, R.; Ashley, G. W.; Santi, D. V. Hydrogel Drug Delivery System Using Self-Cleaving Covalent Linkers for Once-a-Week Administration of Exenatide. *Bioconjug Chem.* **2016**, *27*, 1210−1215.
(20) Beckford Vera, D. R.; et al. PET Imaging of the EPR Effect in Tumor Xenografts Using Small 15 nm Diameter Polyethylene Glycols Labeled with Zirconium-89. *Mol. Cancer Ther* **2020**, *19*, 673−679.

https://doi.org/10.1021/acs.bioconjchem.4c00112
Bioconjugate Chem. 2024, 35, 551−558